Sādhanā Vol. 28, Part 5, October 2003, pp. 897–914. © Printed in India

Controlled wear of vitrified abrasive materials for precision grinding applications

M J JACKSON[1], B MILLS[2] and M P HITCHINER[3]

[1]Cavendish Laboratory, University of Cambridge, Madingley Road, Cambridge, CB3 0HE, United Kingdom
[2]Machining Research Group, Department of Engineering, University of Liverpool, P.O. Box 147, Liverpool, L69 3BX, United Kingdom
[3]Clarendon Laboratory, University of Oxford, Parks Road, Oxford, OX1 3PU, United Kingdom
e-mail: mjjackson@charter.net

Abstract. The study of bonding hard materials such as aluminium oxide and cubic boron nitride (*c*BN) and the nature of interfacial cohesion between these materials and glass is very important from the perspective of high precision grinding. Vitrified grinding wheels are typically used to remove large volumes of metal and to produce components with very high tolerances. It is expected that the same grinding wheel is used for both rough and finish machining operations. Therefore, the grinding wheel, and in particular its bonding system, is expected to react differently to a variety of machining operations. In order to maintain the integrity of the grinding wheel, the bonding system that is used to hold abrasive grains in place reacts differently to forces that are placed on individual bonding bridges. This paper examines the role of vitrification heat treatment on the development of strength between abrasive grains and bonding bridges, and the nature of fracture and wear in vitrified grinding wheels that are used for precision grinding applications.

Keywords. Bonding; aluminum oxide; cubic boron nitride; grinding wheel; wear; precision grinding.

1. Introduction - High efficiency precision grinding

More than twenty-five years of high-speed grinding have expanded the field of application for grinding from classical finish machining to high-performance machining. High-speed grinding offers excellent potential for good component quality combined with high productivity. One factor behind the innovative process has been the need to increase productivity for conventional finishing processes. In the course of process development it has become evident that high-speed grinding in combination with preliminary machining processes close to the finished contour enable the configuration of new process sequences with high performance capabilities. Using the appropriate grinding machines and grinding tools, it is possible to expand the scope of grinding to high efficiency grinding of soft materials. Initially, a basic examination of process mechanisms are discussed that relates the configuration of grinding tools and the requirements of grinding soft materials.

1.1 *Theoretical basis of high efficiency precision grinding*

In view of the random distribution of cutting edges and cutting-edge shapes, statistical methods are applied to analyse the cutting mechanism in grinding. The mean undeformed chip thickness, h_{cu}, and the mean chip length, l_{cu}, are employed as variables to describe the shape of the chip. The undeformed chip thickness is dependent on the static density of cutting edges, C_{stat}, and on the geometric and kinematic variables (Tawakoli 1993),

$$h_{cu} = k[1/C_{stat}]^{\alpha}[v_w/v_s]^{\beta}[a_e/d_{eq}]^{\gamma} \tag{1}$$

where v_w is the workpiece speed, v_s is the grinding wheel speed, a_e is the depth of cut, d_{eq} is the equivalent grinding wheel diameter, and indices α, β, γ are greater than zero. On the basis of this relationship, it can be established that an increase in the cutting speed, assuming all other conditions are constant, will result in a reduction in the undeformed chip thickness. The workpiece material is machined with a larger number of abrasive grain contacts. At the same time, the number of cutting edges involved in the process decreases. This leads to the advantages promised by high-speed grinding which is characterised by a reduction in grinding forces, grinding wheel wear, and in workpiece surface roughness. Consequently, increasing the speed of the grinding wheel can lead to an increase in the quality of the workpiece material, or alternatively, an increase in productivity. The process technology depends on the characteristics and quality requirements of the workpiece to be machined.

As the cutting speed increases, the quantity of thermal energy that is introduced into the workpiece also increases. An increase in cutting speed is not normally accompanied by a proportional reduction in the tangential grinding force, and thus results in an increase in process power. Reducing the length of time the abrasive grain is in contact with the workpiece can reduce the quantity of heat into the workpiece. An increase in the machining rate of the process is necessary for this to happen, where the chip thickness is increased to the level that applies to lower cutting speeds without overloading the grinding wheel.

Experimental results (Tawakoli 1993) illustrate that increasing the cutting speed by a factor of two while maintaining the same metal removal rate leads to a reduction in the tangential force but, unfortunately, leads to an increase in the amount of work done. Owing to constant grinding time, there is an increase in the process energy per workpiece and, subsequently, in the total thermal energy generated. When the material removal rate is also increased the rising tangential force results in a further increase in grinding power. The quantity of thermal energy introduced into the workpiece is lower than the initial situation when the same-machined workpiece volume applies despite the higher cutting speed and increased metal removal rate. These considerations show that machining productivity can be increased using high-speed grinding without having to accept undesirable thermal effects on ground components.

There are three fields of technology that have become established for high-speed precision grinding. These are as below.

- High-speed grinding with *c*BN grinding wheels
- High-speed grinding with aluminium oxide grinding wheels, and
- Grinding with aluminium oxide grinding wheels in conjunction with continuous dressing techniques (CD grinding)

Material removal rates resulting in a super proportional increase in productivity for component machining have been achieved for each of these fields of technology in industrial applications (figure 1). High equivalent chip thickness of between 0·5 and 10 μm are a characteristic feature of high-speed grinding. To achieve a high performance from a grinding wheel it must stay

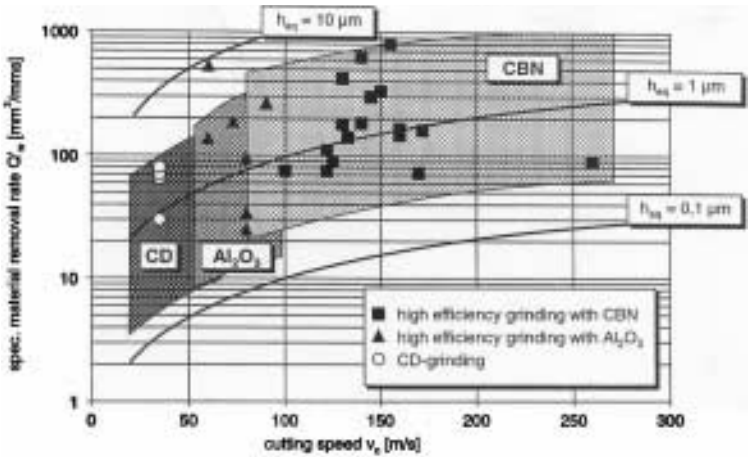

Figure 1. Main field of applications for high efficiency precision grinding.

sharp constantly, and must have the ability to absorb a high volume of metal chips. Therefore, the grinding wheel must be porous and must be able to withstand high grinding loads that are placed on the abrasive grains and on the bonding bridges that hold the grains in position. The nature of the properties of the grinding wheel at the interface between the bonding bridge and the abrasive grains is very important when one considers how forces are transmitted into the bonding bridges through the interfacial layer. Vitrified bonds are typically used for high performance grinding processes and in comparison with other types of bonds, vitrified bonds permit easy dressing while at the same time possess high levels of resistance to wear (Jackson *et al* 1995, 2001). In contrast to impermeable resin and metal bonds, the porosity of the vitrified grinding wheel can be adjusted over a broad range by varying the formulation and the manufacturing process. As the structure of vitrified bonded *c*BN and aluminium oxide grinding wheels results in a subsequently increased chip space after dressing, the sharpening process is simplified, or can be eliminated in numerous applications.

2. Wear of vitrified grinding wheels

The type of grinding wheel considered in this paper is made using aluminium oxide (α-Al_2O_3), a hard material with a Knoop hardness of up to 2000 kg mm^{-2}, is used in the grinding industry in two principal forms: a high purity, fused form of alumina containing over 99·9 wt.% Al_2O_3 that is white in appearance; and a fused, brown coloured, alumina of 95 wt.% purity. The main impurity in this latter form is TiO_2 at a level no greater than 3 wt.%. This tends to increase the toughness of the grain and is accompanied by other impurities such as MgO, CaO, Fe_2O_3, and ZrO_2. Other grinding wheels described in this paper use cubic boron nitride (*c*BN) that has a Knoop hardness in excess of 4500 kg mm^{-2}.

The range of vitreous bonding systems and abrasive types is very large, though only alumino-alkalisilicate and alumino-borosilicate bonding systems are used by the abrasive wheel industry. The normal practice is to adjust the proportions of Al_2O_3, B_2O_3, SiO_2, and alkali oxides to achieve the desired fluidity. Other chemical and physical properties can be modified by the addition of alkaline-earth oxides. Vitreous bonds are composed of mixtures of quartz, feldspar, clay, borate minerals, and ground frits. In practice, the bonds are mixed

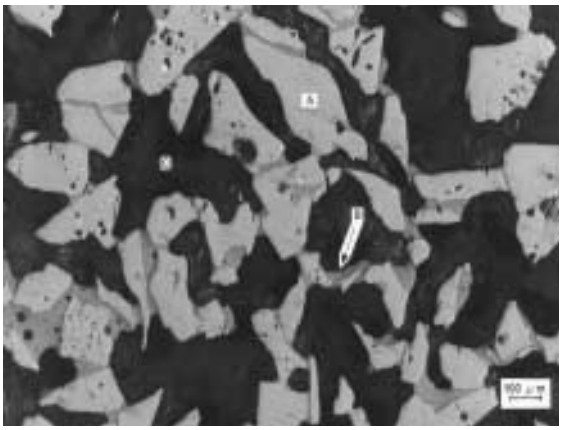

Figure 2. Microstructure of a vitrified grinding wheel. A – denotes abrasive grain, B – denotes vitrified bonding phase, and C – represents distributed porosity.

with a variety of abrasive grains. However, this paper considers high purity and titanium-doped varieties (using a typical mesh size of 220, which is approximately 62 μm diameter abrasive grain size), and cBN with B64 grain size (approximately 63 μm in diameter).

The grinding process is accompanied by wear of the abrasive wheel, and the rate of this wear plays an important role in determining the efficiency of the grinding process and the quality of the workpiece. The structure of a vitrified grinding wheel is composed of abrasive grains, a bonding system, and a large number of pores. Figure 2 shows a typical porous grinding wheel structure (Jackson 2001).

Krabacher (1959) pointed out that wear mechanisms in grinding wheels appear to be similar to that of single-point cutting tools, the only difference being the size of swarf particles generated. The wear behaviour observed is similar to that found in other wear processes; high initial wear followed by steady-state wear. A third accelerating wear regime usually indicates catastrophic wear of the grinding wheel, which usually means that the wheel will need to be dressed. This type of wear is usually accompanied by thermal damage to the surface of the ground workpiece. The performance index used to characterize wheel wear resistance is the grinding ratio, or G-ratio, and is expressed as the ratio of the change in volume of the workpiece ground to the change in the volume of the grinding wheel removed, thus,

$$G = \frac{\Delta v_w}{\Delta v_s} \tag{2}$$

Grinding ratios cover a wide range of values ranging from less than one for vanadium-rich high speed steels to over 60,000 when internally grinding bearing races using cubic boron nitride abrasive wheels. Attempts have been made on how to address the problems related to the wear of abrasive grains in terms of the theory of brittle fracture. The conclusions of various researchers lead us to believe that the variety of different and interacting wear mechanisms involved, namely, plastic flow of abrasive, crumbling of the abrasive, chemical wear etc., makes grinding wheel wear too complicated to be explained using a single theoretical model. High efficiency precision grinding processes place extreme loads onto the grain and the vitrified bonding bridges.

2.1 *Wear mechanisms*

Four distinct wheel wear mechanisms that contribute to the wear of grinding wheels are identified as given below (figure 3).

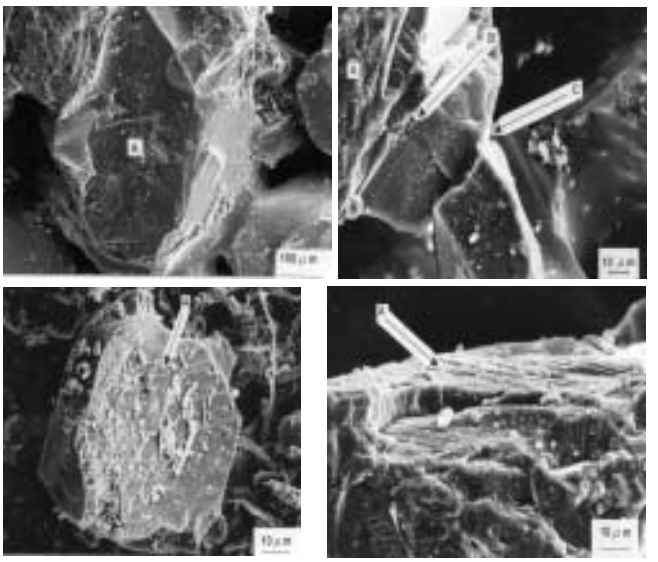

Figure 3. Grinding wheel wear mechanisms: **(a)** abrasive wear; **(b)** bond bridge fracture; **(c)** abrasive grain fracture; and **(d)** interface fracture between abrasive grain and bond bridge.

(a) Abrasive wear (formation of wear flats on the surface of abrasive grains);
(b) fracture of bond bridges;
(c) fracture of abrasive grains due to mechanical and thermal shock loads; and
(d) Fracture at the interface between abrasive grain and bond-bridge.

2.1a *Abrasive wear:* The formation of wear flats on abrasive grains leads to a loss of grain sharpness. The sources of minute scale wear are the following.

(a) Wear due to frictional interaction between workpiece and abrasive grain;
(b) Plastic flow of the abrasive grain at high temperature and pressure;
(c) Crumbling of the abrasive grain due to thermal diffusion and microscale mechanical impact; and
(d) Chemical reaction between abrasive and workpiece material at elevated temperatures and in the presence of grinding fluids.

The latter mechanism can reduce the resistance of the abrasive grain to other wear mechanisms. Dull abrasive grains are caused by the generation of wear flats on active grains that leads to an increase in the area of contact and frictional interactions between abrasive grain and the workpiece. At the point of dulling of the abrasive grain, very high temperatures exist in the area of contact that greatly enhances adhesion and chemical reaction between two surfaces. If grain and bond bridge fracture does not occur during grinding then the plateau area on the grain widens and the rate of wear increases. If fracture is delayed further, as with hard grinding wheels, then the wheel becomes glazed and the workpiece is thermally damaged.

It has been shown experimentally (Geopfert & Williams 1959) that chemical affinity between the abrasive and the workpiece material can be used as a guide for the selection of grinding wheels. Their observations of solid diffusion of silicon carbide into ferrous materials explain the catastrophic wear rates exhibited by these 'wheel-workpiece' combinations. The most common method used for measuring wear flat area employs an optical, or an electron microscope. Hahn (1962) observed and analysed the effect of the increasing wear flat area during the plunge grinding of various workpiece materials. Hahn concluded that grinding

forces gradually increase during wear-flat formation up to a point where the grinding wheel will restore its sharpness due to abrasive grain fracture.

2.1b *Fracture wear:* The occurrence of abrasive grain and bond fracture are considered simultaneously for the following reasons.

(a) They are of the same nature, i.e. fracture of brittle materials and hence the theory of brittle fracture is applicable to both bonding bridge and abrasive grain. The applied thermal and mechanical loads, usually under cyclic conditions, cause initiation and further development of cracks that leads to fracture and the formation of new irregular surfaces;
(b) they are related to dressing methods used and occur simultaneously. The initial and final stages of wheel life between dressings exhibit fracture wear that is a combination of abrasive grain and bonding bridge fracture;
(c) the relative amounts of bond bridge and abrasive grain wear cannot always be calculated. An investigation into precision grinding employed a soft wheel that gave a high percentage of bond fracture, whereas a harder wheel gave partial abrasive grain fracture. Wear by attrition occurred in both cases.

However, the combination of grinding parameters such as equivalent chip thickness and the grindability of the workpiece material determines the effective wheel hardness, and so no single feature of the grinding process can be used to predict the fracture pattern of the wheel in advance. The difficulty when relating grinding wheel wear due to fracture to a particular grinding condition arises from the lack of knowledge about the loads applied to both abrasive grains and their bonding bridges and their response to these applied loads.

Tarasov (1963) suggests that abrasive grain fracture occurs as a result of mechanical forces due to chip formation, or thermal shock, induced by instantaneously high temperatures. Hahn (1962) proposed a thermal stress hypothesis to explain the fracture of abrasive grains. Plunge grinding experiments were conducted under fixed normal load conditions. Hahn asserted that as wear progresses measurements of torque indicated that the tangential force decreases. This led to the conclusion that abrasive grain fracture due to mechanical loading will not occur. Mechanical stresses wear also considered as an explanation for the different rates of wear of the grinding wheels used in the experiments.

Bhattacharyya *et al* (1965) observed abrasive grain loss due to fracture using an electron microscope. They concluded that they could not differentiate between Peklenik's crystal splintering, i.e. grit flaking due to thermal stress, and abrasive grain fragmentation. However, they did explain their results in terms of Hahn's thermal shock hypothesis. Hahn's experimental conditions suggested that attrition of the abrasive was expected to occur through abrasive wear. Wear measurements by Hahn (1962) were based on the reduction in grinding wheel diameter, which Malkin & Cook (1971) attributed to abrasive wear. Wear rates recorded were of the order of 50 microinches per second. It was expected that abrasive wear rates were in the region of 5 microinches per second. This rate was observed under light grinding conditions. Under heavy grinding conditions, the conditions of wear appeared to be more complex.

Malkin & Cook (1971) collected wheel wear particles for each grade of grinding wheel when grinding using a fixed set of operating conditions. They analysed their size distributions statistically and discovered that a soft-grade grinding wheel (G-grade) produces 85% of grinding debris associated with bonding bridge fracture, whilst a harder-grade grinding wheel (K-grade) produces 55% of grinding debris associated with fractures of bonding bridges. Abrasive wear accounted for 4% of the total wear in both cases.

The strongest evidence in support of the idea of fracture due to mechanical loading is that fracture occurs some distance away from the cutting edge (Jackson 2002). It was concluded that the heat generated by cutting has no effect on abrasive grain fracture since the peak temperature of the abrasive grain occurs at the surface of the grain in contact with the workpiece where fracture is initiated on cooling according to the thermal stress hypothesis. The hypothesis does not take account of any difference in the coefficient of thermal expansion between abrasive grain and bond bridges, and also the effect of thermal shocks on the quenching action of grinding fluids on the abrasive grain leaving the cutting zone. The latter case was analysed and it was reported that the thermal stress in an abrasive grain due to a pulsating heat source showed that the magnitude of the maximum tensile stress is not large enough to cause fracture of the grain. Malkin & Cook (1971) adopted the mechanical loading approach, and derived an expression from first principles for the probability of bond fracture in terms of a bond stress factor.

Although bond and grain fracture are similar mechanisms, they have a different effect on the economics of the grinding process. The first mechanism results in a rapid loss of the grinding wheel, while the second mechanism, on a comparable scale with the un-cut chip thickness, generates sharp cutting edges and is known as the 'self-dressing action'. Both mechanical and thermal stresses appear to be responsible for fracture wear. The effect of heat at the abrasive grain and workpiece interface is responsible for locally affecting the mechanical properties of the abrasive grain. However, fragments of larger sizes of abrasive grain are more likely to occur through mechanical loading that governs bond fracture and the self-sharpening action. A method of alleviating the onset of bond fracture due to unusually large mechanical loads is to dissolve deleterious particles in the bonding system that weakens the structure of the bonding bridge. In vitrified bonds, these particles are quartz particles that naturally occur in ceramic raw materials. These particles reduce the load-bearing strength of the bonding bridges during vitrification heat treatment.

The study of the effect of the elastic modulus on the fracture behaviour of vitrified abrasive grinding wheels was conducted by Decneut *et al* (1970). They discovered that vitrified grinding wheels with a high modulus of elasticity wear by a mechanism of abrasive grain fracture rather than fracture of the glass bond bridges that hold the abrasive grains in place. As the modulus of elasticity increases the 'self-sharpening effect' is lost because abrasive grains cannot be released from the bonding matrix. This leads to a condition where the temperature of the workpiece material begins to increase and is associated with phase transformations and thermal cracking of the surface layers that results in a reduction in fatigue strength. In this case, the performance of the abrasive grinding wheel for a specific metal removal rate and workpiece material depends on the selection of the appropriate grade of abrasive grinding wheel that is a function of its modulus of elasticity and strength. In the present study, the elastic modulus, bending strength, and nature of fracture was found to be dependent on the vitrification behaviour of the glass bonding system, the amount of bond, and the type of abrasive grain used in the vitrified grinding wheel. It was found that the wear of vitrified grinding wheels is highly dependent on the way the grinding wheel 'vitrifies' during heat treatment.

3. Microstructure of abrasive grains

3.1 *High purity aluminium oxide*

Examination of high purity aluminium oxide in a scanning electron microscope using an electron probe micro analyzer showed that 99·5 wt.% of the grain was Al_2O_3 with the balance

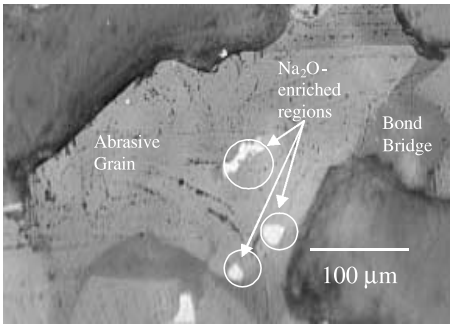

Figure 4. High purity aluminium oxide grinding wheel showing enriched regions of Na_2O determined using an electron probe micro analyser.

consisting of Na_2O and SiO_2 in equal proportions. However, local Na_2O-enriched areas were observed within parts of the grain. Figure 4 shows the areas of Na_2O local enrichments within the grain as white reflections when viewed under an optical microscope.

Under close examination, high purity aluminium oxide contains aluminium oxide, sodium aluminate, carnegieite, sodium monoaluminate, nepheline, and glass of variable composition. In heat-treated high purity abrasive grains, preferential etching at the surface of the grain appears to occur along crystallographically controlled directions (figure 5). This is assumed to be due to the dissolution of planar blocks of β-Al_2O_3($Na_2O{\cdot}11Al_2O_3$) that is present in the α-Al_2O_3 host material. X-ray diffraction of high purity alumina established the existence of β-Al_2O_3 prior to the optical examination of the abrasive grains.

Other impurities found include rarely seen calcium rich platelets in the form of alite (Ca_3SiO_5), and an un-named oxide, $NaCaAlO_3$, which is known to have several polymorphic forms.

3.2 *Titanium-doped aluminium oxide*

The amount of TiO_2 in titanium-doped aluminium oxide was measured using an electron probe and was found to be in the range of 1 to 2 wt.%. The amount of titania present is inconsistent with earlier work that had determined that the maximum solubility of TiO_2 in Al_2O_3 is less than 0·3 mol.% at 1300°C (Winkler *et al* 1966). Although some of the excess can be accounted for in the formation of Ti_2O_3, It is possible that not all titania is in solid solution. This was confirmed by the occurrence of blade-like inclusions that is consistent with rutile (TiO_2) needle morphology. This would account for the variability in measured titania and its

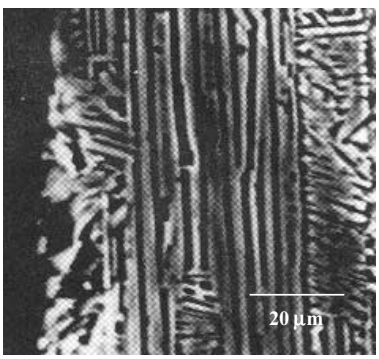

Figure 5. High purity aluminium oxide grain showing thermally etched channels of β-Al_2O_3 layers that are present in the α-Al_2O_3 structure.

presence in amounts greater than its solubility in Al_2O_3. In heat-treated and titanium-doped aluminium oxide, calcium hexaluminate, anorthite, and spinel are not affected by the heat treatment process. However, glass is devitrified forming anorthite spores. Titanium minerals are oxidised to higher oxides such as anatase and rutile. These changes are accompanied by large changes in volume that may affect the performance of any abrasive tool. As a precaution, Ti-doped aluminium oxide must be heated to 1000°C before it can be used for making abrasive cutting tools.

3.3 *Cubic boron nitride*

Cubic boron nitride (*c*BN) abrasive grains are made by compacting grains of *c*BN in the presence of aluminium. Aluminium reacts with BN to form a mixture of AlN and AlB_2 that forms a stable and catalytically inactive binder. Interaction between aluminium and BN is intimate and can be observed directly using scanning and transmission electron microscopes. There is very little interaction between *c*BN grains. The edges of *c*BN grains not in contact with each other form rinds of AlN in thin, continuous lines with several nodules along its length. The rind that encloses the exposed *c*BN grain is always orientated so that it has crystallographic directions parallel to a particular directions in the *c*BN lattice. The selected area diffraction pattern shown in figure 6 shows a [110] *c*BN pattern with a rectangular AlN[11$\bar{2}$0] pattern superimposed. The AlN has grown with its basal planes parallel to the *c*BN facet plane. This orientation with *c*BN (110) // AlN (0001) and *c*BN [110] // AlN [11 0] is the most common orientation observed even when facet planes deviate away from being octahedral. At cube surfaces the orientation the orientation *c*BN (001) // AlN (0001) and *c*BN [110] // AlN [11$\bar{2}$0] occurs. While most of the AlN can be located at *c*BN grain surfaces, AlB_2 nucleates independently in liquid aluminium at the later stages of consolidation. A single

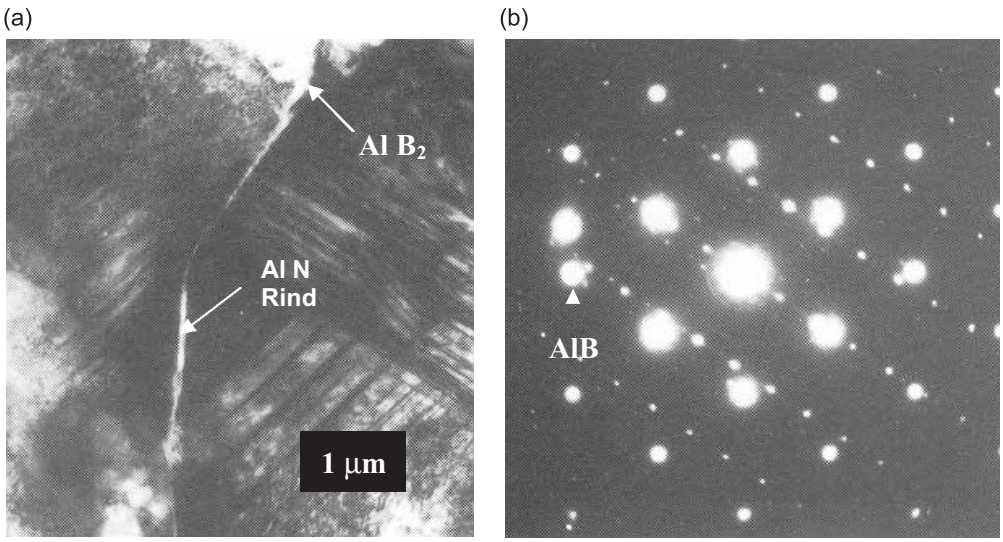

Figure 6. **(a)** Two contacting *c*BN grains separated at intervals by an AlN rind which is parallel to the *c*BN [110] planes. The outer edges of the grains are in contact with a featureless AlB2 layer, **(b)** Selected area diffraction pattern from part of the field of contact showing the relative orientation of phases present. The smaller spots are AlN, and the larger spots are *c*BN. The arrow indicates the single spot generated by AlB_2 phase.

crystal of AlB2 produces the reflection to the left of the SAED pattern that produces a single bright spot (Walmsley & Lang 1988).

4. Experimental procedures

4.1 *Measurement of mechanical properties*

The experimental procedure involved making experimental samples of abrasive grain and glass bond as a vitrified product using high purity aluminium oxide, titanium-doped aluminium oxide, and *c*BN bonded with an alumino-borosilicate bond containing 61·4 wt.% SiO_2, 17 wt.% Al_2O_3, 0·4 wt.% Fe_2O_3, 3·2 wt.% CaO, 0·1 wt.% MgO, 2·7 wt.% Na_2O, 3·1 wt.% K_2O, and 10·1 wt.% B_2O_3.

Experimental samples were made by pressing abrasive grains and glass bond ingredients to a known density. The samples were moulded in the form of bars. The dimensions of the bars were sixty millimetres' length, twelve millimetres' height, and twelve millimetres' depth. The samples were fired at the vitrification temperature (between 1000°C and 1300°C) for six hours in an electric furnace. The samples were prepared for four-point loading and for measuring their elastic modulus using the sonic method developed by Decneut *et al* (1970). A total of twenty experimental test samples were loaded in uniaxial tension.

The Weibull modulus for the fractured samples was calculated to be 18·3 for aluminium oxide samples, and 18·8 for *c*BN samples. A section of one of the bar samples was cut, mounted in resin, and polished to reveal the nature of bonding between glass and aluminium oxide. Figure 7 shows the section revealing abrasive grains bonded together by the vitrified glass bonding system. The black areas represent the pores between abrasive grains that are essential to provide free space for chips of metal and for coolant access. Figure 7 also shows the characteristic x-ray spectra for abrasive grains and glass bond. The abrasive grain spectrum shows aluminium and titanium (indicative of titanium-doped aluminium oxide), and the glass bond spectrum shows elements such as potassium, calcium, and sodium that are glass network-modifying elements, and aluminium and silicon that are network-forming elements. For the

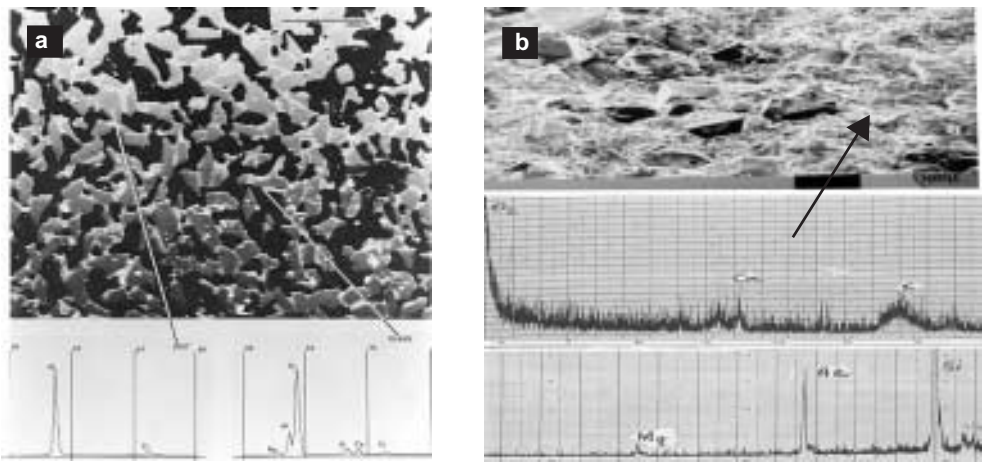

Figure 7. Electron probe microanalysis of **(a)** titanium-doped aluminium oxide and vitrified glass bonding system, and **(b)** *c*BN and vitrified glass bonding system.

vitrified *c*BN grinding wheel, the bonding system contains magnesium, aluminium, silicon, calcium, and oxygen.

4.2 *Manufacture of grinding wheels*

Grinding wheel segments were made by pressing abrasive grains and glass bond ingredients to a known density. The samples were moulded in the form of segments to be attached to a pre-balanced grinding wheel body. The dimensions of the Segments were sixty millimetres' length, fifteen millimetres' height, and twenty millimetres' depth. The samples were fired at the vitrification temperature (between 1000° and 1300°C) for six hours in an electric furnace. Once fired, the segments were measured in terms of their hardness and grade and were bonded onto a steel backing using a high strength adhesive. The steel backings were then bolted onto a steel body containing the rest of the abrasive segments.

4.3 *Measurement of wear*

The method of grinding wheel wear measurement adopted was the 'razor-blade' technique. The method involves grinding a workpiece that is less wide than the grinding wheel. A groove is worn into the wheel profile, which was measured with reference to the non-grinding portion of the grinding wheel using a razor blade. The grinding wheel was initially dressed using a single point diamond and the wheel conditioned until steady-state grinding wheel wear was achieved. In order to achieve the conditions of bond fracture, the depth of cut for all experiments was set at 10 μm per pass with a table speed of 0·2 m/s, and a grinding wheel speed of 60 m/s. Immediately after the grinding experiments were performed, the razor blade was then lowered into the grinding position with the grinding wheel touching the blade. After grinding the blade, the wear of the grinding wheel was measured using a surface profilometer. The grinding ratio was calculated by measuring the volume of the grinding wheel removed, and the volume of the workpiece removed, (2).

5. Experimental results

5.1 *Mechanical properties*

The relationship between the elastic modulus and firing temperature as a function of abrasive grain type and bonding content is shown in figure 8 for both high purity and titanium-doped aluminium oxide structures. It is shown that the elastic modulus is developed as the vitrification temperature is increased, and is highly dependent on the amount of bonding material that surrounds the abrasive grain.

This is confirmed in figure 9, which shows the effect of the increase in bonding content on the elastic modulus at three different vitrification temperatures for high purity aluminium oxide structures. An interesting observation is that up to the softening point of the glass bond, high purity and titanium-doped aluminium oxide vitrified structures developed strength in the same way then declines for titanium-doped aluminium oxide structures depending on the amount of bonding material. The relationship is shown in figure 10. The same general trends are observation with vitirified *c*BN grinding wheels.

5.2 *Wear of grinding wheels*

The relationship between the wheel wear parameter, grinding ratio (G), and the firing temperature is shown in figure 11 for both high purity and titanium-doped aluminium

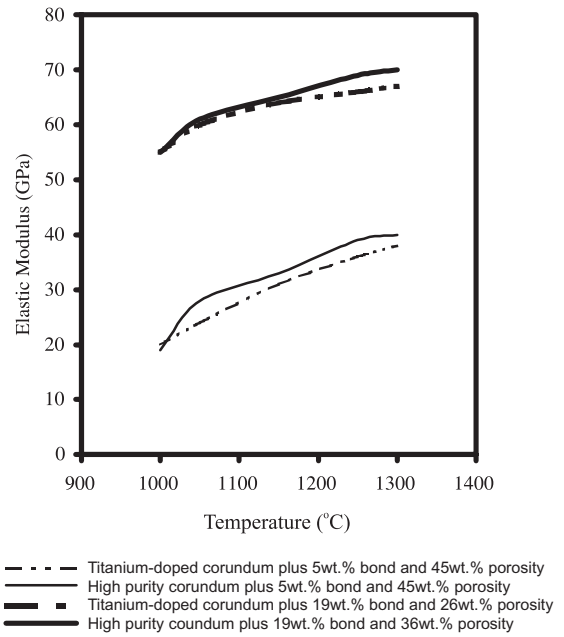

Figure 8. Elastic modulus as a function of firing temperature for a number of abrasive grain types and bond contents.

oxide grinding wheel structures containing a different amount of vitrified bonding material. Again, the observation that up to the softening point of the glass bond, high purity and titanium-doped aluminium oxide structures develop wear resistance in the same way is noteworthy.

Figure 11 shows that the grinding ratio is a function of vitrification temperature, but at a certain temperature, it is highly dependent on the type abrasive grain used in the grinding wheel and the amount of bonding material used.

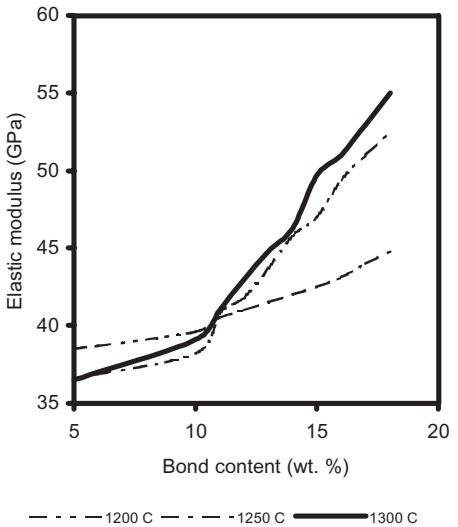

Figure 9. Effect of bond content and firing temperature on the elastic modulus of high purity aluminium oxide structures.

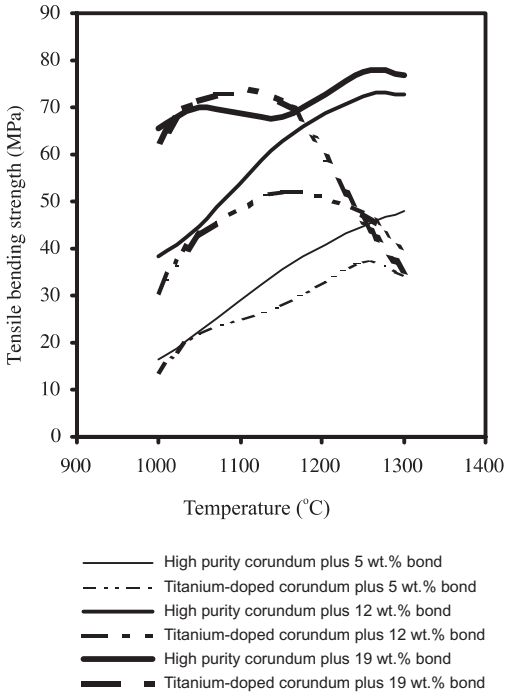

Figure 10. Relationship between bending strength and firing temperature as a function of abrasive grain type and bond content.

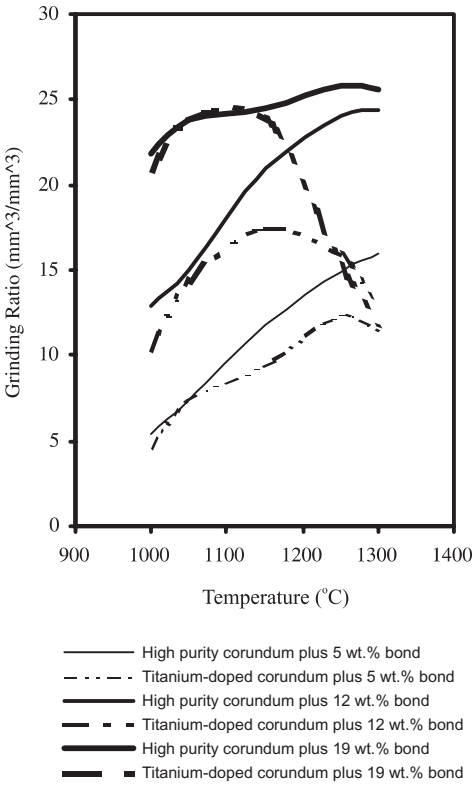

Figure 11. Relationship between grinding ratio and firing temperature as a function of abrasive grain type and bond content.

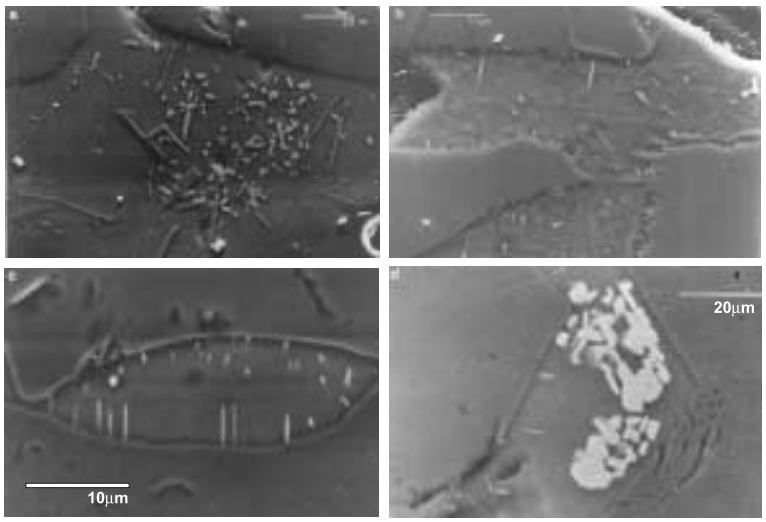

Figure 12. **(a)** Titania (TiO_2), in the form of rutile needles, on the surface of the vitrified glass bond; **(b)** vitrified glass bond etched with 40% HF in water to show rutile formation within the glass bonding system; **(c)** electron backscattered image showing needle growth into the glass bond from the abrasive; **(d)** de-vitrified glass bond containing crystals of $Al_{18}B_4O_{33}$ bounded by two abrasive grains.

Examination in a scanning electron microscope showed that certain parts of the glass bond had de-vitrified in both high purity and titanium-doped aluminium oxide structures. The crystals are elongated with square sections and have a high Al_2O_3 content. An x-ray diffraction spectrum indicated that the phase is an aluminoborate solid solution. The best match was with $Al_{18}B_4O_{33}$. In addition to this phase, a second crystalline phase was observed in titanium-doped aluminium oxide structures. The phase consists of needles of rutile (TiO_2) orientated on the faces of titanium-doped aluminium oxide grains that penetrate into the glass bond. Figures 12a and b shows orientated rutile needle formation in the glass bond emanating from the aluminium oxide crystals. The structure in figure 12b was etched with a solution of 40% hydrofluoric acid in water. Figure 12c shows the growth of rutile needles from the interface between aluminium oxide and the glass bond using the electron backscatter mode. Figure 12d shows the de-vitrification of glass in the form of $Al_{18}B_4O_{33}$ crystals.

Fractured samples revealed a higher proportion of intergranular fracture than cut and polished samples. High purity aluminium oxide did not exhibit intergranular fracture at the interface between abrasive and bond but did exhibit the bond fracture mode. It appears that titania is an undesirable constituent in bonding systems that tends to promote interfacial fracture at the abrasive grain-bond bridge interface. Even if its presence does not cause a reduction in cohesive strength, one method of reducing its effect is for it to form a titanate compound that does not reduce interfacial strength. Examination of fractured high purity aluminium oxide samples revealed preferential etching of the abrasive grain by the glass bond. This is assumed to be dissolution of blocks of β-aluminium oxide ($Na_2O{\cdot}11\ Al_2O_3$) present in α-aluminium oxide (pure aluminium oxide).

The relationship between the wheel wear parameter, grinding ratio, and the firing temperature for vitrified *c*BN grinding wheel structures containing different amounts of bonding content is shown in figure 13. An interesting observation one can observe is that the retention of the abrasive grains in the vitrified bonding matrix can be improved by increasing the sin-

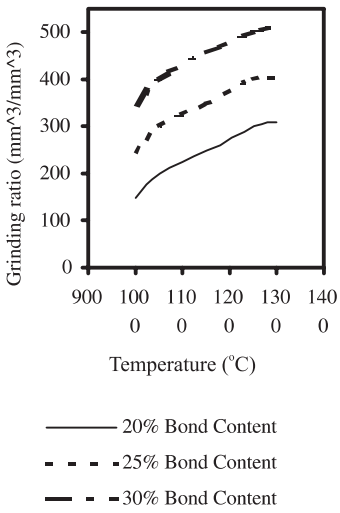

Figure 13. Relationship between grinding ratio and firing temperature as a function of bond content for vitrified *c*BN grinding wheel structures.

tering temperature. In order to investigate the mechanism of *c*BN retention, samples of the post-fired abrasive structures were polished and etched.

Figure 14 shows the unpolished fracture surfaces of the vitrified *c*BN grinding wheels. A magnified image of the interface between abrasive grain and bonding bridge is shown in Figure 14b. Interfacial cohesion appears to be quite apparent in this image. Figure 15 shows a polished and etched fracture surface in the vicinity of the abrasive grain and bonding bridge. The associated electron probe microanalysis of the image clearly shows a concentration of oxygen at the interface between *c*BN and glass bonding bridge. The concentration of oxygen appears to be associated with boron and the formation of a boron-containing oxygen layer that separates the alumino-borosilicate bonding system and the cubic boron nitride abrasive grain. This is thought to be a relatively thin layer of B_2O_3 (boric oxide). As the sintering temperature is increased, the thickness of this layer is also increased with a subsequent loss of boron from the abrasive grain. Figure 16 illustrates the relationship between the interfacial layer thickness and sintering temperature. As the temperature is increased further, the width of the interfacial layer tends to stabilize and reaches an equilibrium thickness.

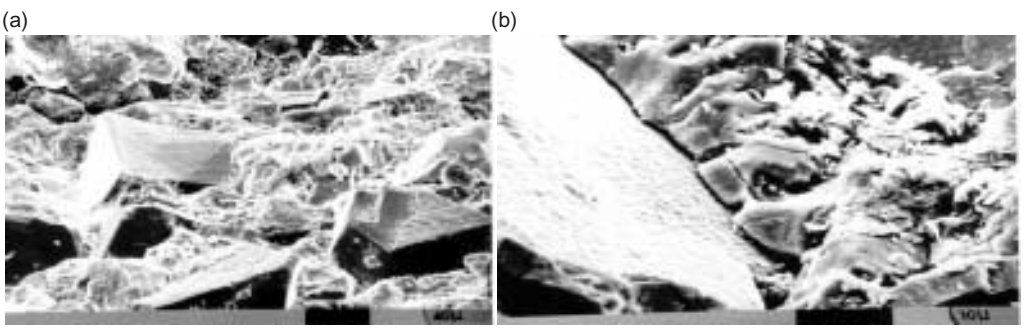

Figure 14. **(a)** Vitrified *c*BN grinding wheel structure, **(b)** interface between *c*BN abrasive grain and vitrified bonding.

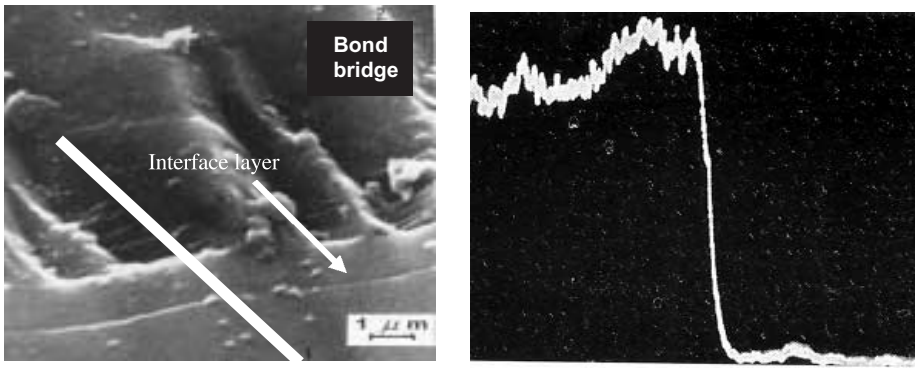

Figure 15. **(a)** Polished cross section of *c*BN abrasive and bond bridge clearly showing the interface layer, **(b)** electron probe microanalysis of oxygen across the line scan shown in (a), left-to-right.

6. Discussion

The existence of β-aluminium oxide was established by X-ray methods. When the bond content is low in samples made with high purity aluminium oxide, failure occurs by fracture of bonding bridges. At higher bond contents the mode of failure is one of abrasive grain fracture. Fracture at the abrasive grain-bond bridge interface was not observed. This is because the β-aluminium oxide phase is etched away preferentially due to the dissolution of Na_2O into the glass bond that locally increases the fluidity of the bond. This allows the bond to penetrate the surface of the abrasive grain and provides it with enhanced shear resistance.

This effect does not happen with titanium-doped aluminium oxide, in fact, the strength decreases at the softening point of the glass because of enhanced dissolution of aluminium oxide that releases more TiO_2 into the glass bond for rutile needle growth. Therefore, in

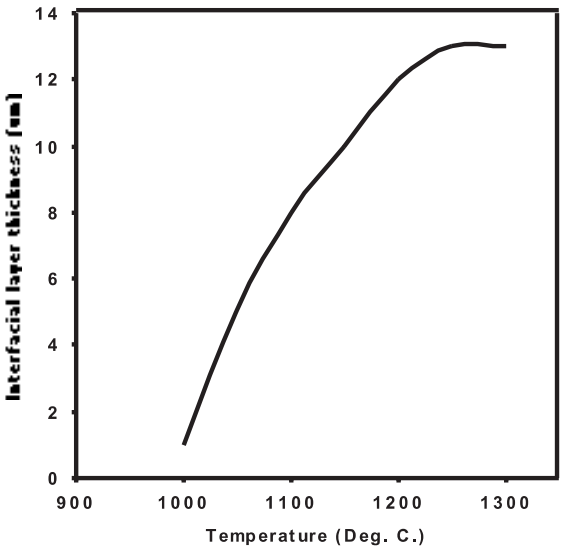

Figure 16. Interfacial layer thickness between *c*BN and vitrified bonding bridge as a function of sintering temperature.

contrast to Decneut *et al* (1970) the mode of fracture in titanium-doped structures is interfacial between abrasive grain and glass bond and is not completely dependent on bond content.

Even in the case where bond bridges have preferentially fractured, the mode of fracture is always associated with rutile needle weakening. The vitrification temperature and glass bond content has a significant effect on the elastic modulus of high purity and titanium-doped aluminium oxide structures. The differences in strength between these structures when fired at temperatures above the softening point of the glass bond is due to differences in the crystal structures of the two types of abrasive grain. The presence of β-aluminium oxide in high purity aluminium oxide allows selective dissolution of aluminium oxide to occur that enables stronger bonding to take place between aluminium oxide and glass. This effect does not happen with titanium-doped aluminium oxide where dissolution allows the precipitation of TiO_2 into the glass bond in the form of rutile needles that reduces the cohesive strength between aluminium oxide and glass.

The existence of an interfacial layer between *c*BN and glass was thought to be that of the formation of boric oxide (B_2O_3). As sintering continued, the layer became thicker and tended to strengthen the interfacial layer. This is assumed to be the reason why the grinding ratio of the abrasive tool increased as a function of sintering temperature. It was also noted that the size of the *c*BN grains decreased as sintering temperature increased until an equilibrium interfacial layer thickness was reached. It would also be right to assume that at this point, that diffusion of oxygen into the *c*BN abrasive grain ceases to occur. The fracture surface of the vitrified *c*BN structure shows that fracture is associated with fracture within the bonding bridge rather than fracture at the *c*BN-bond bridge interface. This tends to imply that the interfacial bonding layer is stronger than bonding bridge.

7. Conclusions

The behaviour of abrasive cutting tools is dependent on the type of abrasive grain used, its heat treatment schedule, and its bond content. The vitrification behaviour is dependent on certain processing variables and the bonding systems used for precision grinding wheels. It is evident that rutile needles have a significant effect on the mechanical properties and the behaviour of conventional abrasive cutting tools. If titanium-doped aluminium oxide is used as the cutting medium then heat treatment cycles should be designed that prevent the growth of the needles into the bonding system.

Vitrified *c*BN grinding wheels tend to fracture at the bond bridge rather than at the interface between *c*BN and its glass bonding bridge. This implies that the relatively thin layer of boric oxide is stronger than the bonding bridge material.

The authors thank Professor Mick Brown, FRS, for use of the scanning and transmission electron microscopes at the Cavendish Laboratory, University of Cambridge, and Professor David Tabor, FRS, on discussions on machining and the nature of wear during machining operations.

References

Bhattacharyya S K, Grisbrook H, Moran H 1965 Analysis of grit fracture with changes in grinding conditions. *Microtechnic.* 22: 114–116

Decneut A, Snoeys R, Peters J 1970 Sonic testing of grinding wheels. Report MC 36, November 1970, Centre de Recherces Scientifiques et Techniques de L'industrie des Fabrications Metalliques, University of Louvain, Belgium

Geopfert G J, Williams J L 1959 The wear of abrasives in grinding. *Mech. Eng.* 81: 69–73

Hahn R S 1962 On the nature of the grinding process. *Proc. 3rd Int. Machine Tool Design and Research Conference* (Manchester: Pergamon) pp 129–154

Jackson M J 2001 Vitrification Heat Treatment during the manufacture of corundum grinding wheels. *Trans. ASME. - J. Manuf. Process.* 3: 17–28

Jackson M J 2002 Wear of perfectly sharp grinding wheels. *Trans. North Am. Manuf. Res. Inst. Soc. Manuf. Eng.* 30: 287–294

Jackson M J, Barlow N, Mills B, Rowe W B 1995 Mechanical design safety of vitreous-bonded cylindrical grinding wheels. *J. Inst. Mater. Br. Ceram. Trans.* 94: 221–229

Jackson M J, Barlow N, Hon K K B 2001 Computer aided design of high-performance grinding tools. Proceedings of the Institution of Mechanical Engineers, Part B. *J. Eng. Manuf.* 215: 583–588

Krabacher E J 1959 Factors influencing the performance of grinding wheels. *Trans. ASME, J. Eng. Ind.* 81: 187–200

Malkin S, Cook N H 1971 The wear of grinding wheels - Part 1: Attritious wear. *Trans. ASME - J. Eng. Ind.* 93: 1120–1128

Tarasov L P 1963 Grinding wheel wear grinding tool steels. *Int. Res. Prod. Eng. - Am. Soc. Manuf. Eng.* 21:196

Tawakoli T 1993 High efficiency deep grinding (London: Professional Engineering Publishers)

Walmsley J C, Lang A R, Barrett C 1988 Transmission electron microscope study of syndax 3 compared with syndite and amborite. *Adv. Ultrahard Mater. Appl. Technol.* 4: 61–75 (De Beers Industrial Diamond Division, UK)

Winkler E R, Sarver J F, Cutler I B 1966 Solid solution of titanium dioxide in aluminium oxide. *J. Am. Ceram. Soc.* 49: 634–637